Research in Astron. Astrophys. **2013** Vol. **13** No. **7**, 849–861
http://www.raa-journal.org *http://www.iop.org/journals/raa*

Research in Astronomy and Astrophysics

A revised rotation curve of the Milky Way with maser astrometry *

Xiao-Sheng Xin and Xing-Wu Zheng

School of Astronomy and Space Science, Nanjing University, Nanjing 210093, China; *xwzheng@nju.edu.cn*

Received 2012 December 30; accepted 2013 March 5

Abstract We reconstruct the rotation curve of the Milky Way using the new trigonometric parallax and proper motion data for masers in 43 high-mass star-forming regions obtained by VLBI, as well as the existing data from the literature, based on a new set of galactic constants $(R_0, \Theta_0) = (8.4\ \mathrm{kpc}, 254\ \mathrm{km\,s^{-1}})$ measured by Reid et al. The revised rotation curve of the Milky Way is almost flat or slightly rising in the region from about 6 to 15 kpc. The rotation velocities within 5 kpc of the Galactic center, as determined by VLBI, differ from those obtained by measurement of the HI- and CO-line tangent velocities. We fitted the revised rotation curve arising from three mass components: the bulge, disk and dark matter halo. The total mass of the Milky Way is found to be $2.3\times10^{11}\ M_\odot$ (20 kpc). This is about 10% larger than that from Sofue et al, and is comparable with the mass of M31, $3.4\times10^{11}\ M_\odot$ (35 kpc), given by Carignan et al. The limited accurate observational data, especially the VLBI data, do not permit a fully satisfactory fit to the rotation curve. The extensive parallax and proper motion data that will be produced by the Bar and Spiral Structure Legacy Survey project in the next few years should lead to considerable progress in understanding the rotation curve and dark matter halo of the Milky Way.

Key words: Galaxy: structure — Galaxy: bulge — Galaxy: disk — Galaxy: halo — dark matter — masers

1 INTRODUCTION

Galactic rotation curves are important tools in studies of the structure and mass distribution of galaxies. The flatness of the outer rotation curves implies that galaxies contain large amounts of dark matter. For the Milky Way, the rotation curve is supposed to be the most direct and effective way to study the properties of dark matter, such as its size, mass and distribution.

Many methods have been used to characterize the rotation curve of the Milky Way, such as tangent velocities in the inner Galaxy (Burton & Gordon 1978; Clemens 1985; Fich et al. 1989), the optical distances and CO-line radial velocities of HII regions (Fich et al. 1989), the HI thickness for the entire Galactic disk (Merrifield 1992; Honma & Sofue 1997), and the optical distances and radial velocities of C stars (Demers & Battinelli 2007). These data define a rotation curve of the Milky Way out to $\sim$20 kpc from the Galactic center (GC). As in other galaxies, the Milky Way

∗ Supported by the National Natural Science Foundation of China.

shows a flat rotation curve, with no Keplerian decline. Although different theoretical interpretations are possible, the hypothesis that the flat rotation curve arises from a dark matter halo has been widely accepted. However, we identify three issues concerning the determination of the rotation curve of the Milky Way.

(1) Different authors use different target objects with different errors to construct the rotation curve of the Milky Way.
(2) The kinematic distance is adopted for gaseous objects. This distance is based on purely circular motions around the GC, but we know that many Milky Way objects have significant non-circular motions, which may cause scatter in the measurement of the rotation curve.
(3) A correct rotation curve of the Milky Way relies on two Galactic parameters: the distance of the Sun from the GC, R_0, and the rotation velocity of the local standard of rest (LSR), Θ_0. However, these two fundamental parameters remain remarkably uncertain.

These problems may be resolved by the Bar and Spiral Structure Legacy (BeSSeL) Survey, a Very Long Baseline Array (VLBA) science project named in honor of Friedrich Wilhelm Bessel who first measured stellar parallax. In this project, about 500 high-mass star-forming regions (HMSFRs) in the spiral arms of the Milky Way will be observed by the VLBA in the maser lines of hydroxyl (OH), methanol (CH_3OH) and water (H_2O). The trigonometric parallaxes and proper motions of these regions will be determined with $\sim$10 μas and $\sim$1 km s^{-1} accuracy. The trigonometric parallax is the most fundamental method for stellar distance measurement, since it is based on pure geometry without astrophysical assumptions. Thus the BeSSeL Survey will result in accurate measurements of the distances and three-dimensional velocities of most galactic HMSFRs visible from the northern hemisphere, and will determine fundamental parameters such as R_0 and Θ_0 with approximately 1% accuracy. The uniformity of the targets, instruments and data analysis all aid in the construction of a reliable rotation curve of the Milky Way. Combined with other observations, this should yield the real distribution of mass among the various components of the Milky Way, including the dark matter halo.

In preparation for the BeSSeL Survey, the VLBA has measured trigonometric parallaxes and proper motions for 10 methanol (12 GHz) masers in HMSFRs (Reid et al. 2009a; Moscadelli et al. 2009; Xu et al. 2009; Zhang et al. 2009; Brunthaler et al. 2009). Reid et al. (2009b), combining these results with eight other sources with H_2O or SiO masers measured with the Japanese VLBI Exploration of Radio Astronomy (VERA) and with methanol, H_2O or continuum emission measured with VLBA (Reid et al. 2009b and references therein), fit a model of the dynamics of the Milky Way to estimate the distance to the GC $R_0 = 8.4 \pm 0.6$ kpc and rotation velocity $\Theta_0 = 254 \pm 16$ km s^{-1} at the Sun.

In this paper, we present a tentative new rotation curve of the Milky Way using the existing data in the literature and recent maser astrometry by the VLBA, VERA and European VLBI Network (EVN) (Ando et al. 2011; Honma et al. 2011; Hirota et al. 2011; Imai et al. 2011; Kurayama et al. 2011; Moscadelli et al. 2011; Niinuma et al. 2011; Oh et al. 2010; Rygl et al. 2010; Rygl et al. 2012; Sanna et al. 2009; Sanna et al. 2012; Sato et al. 2010; Tafoya et al. 2011; Xu et al. 2011 and Reid et al. 2009b and references therein). In Section 2 we present our compilation of data from the literature, recalculated with the new Galactic constants proposed by Reid et al. (2009b). The revised rotation curve of the Milky Way that we obtain is then fitted to our mass model in Section 3. The results on the mass distribution and properties of the Milky Way and its dark matter halo are presented in Section 4. The conclusions and future prospects are then given in Section 5.

2 DATA REDUCTION AND THE NEW ROTATION CURVE OF THE MILKY WAY

We first recalculate the existing data in the literature using the new Galactic constants $(R_0, \Theta_0) = (8.4 \text{ kpc}, 254 \text{ km s}^{-1})$ (Reid et al. 2009b). These results can then be combined with the VLBA, VERA and EVN measurements to produce our revised rotation curve of the Milky Way.

The tangent velocity data of the HI line in the Galactic central region (Burton & Gordon 1978) and CO line in the inner Galaxy, both compiled by Clemens (1985), are corrected by

$$R_{\rm c} = R_i + \Delta R_0 \frac{R_i}{R_0}, \tag{1}$$

$$\Theta_{\rm c}(R_{\rm c}) = \Theta_i(R_i) + \Delta\Theta_0 \frac{R_i}{R_0}\,, \tag{2}$$

in which R_i and Θ_i are the solar distance to the GC and the rotation velocity used by Clemens (1985), respectively. $\Delta R_0 = -0.1$ kpc and $\Delta\Theta_0 = 34$ km s^{-1} are corrections for the solar distance and rotation velocity, and $R_{\rm c}$ and $\Theta_{\rm c}$ are the final corrected values.

The HI tangent velocity data for $l = 15^\circ\sim90^\circ$ and $l = 270^\circ\sim345^\circ$ in Fich et al. (1989) are taken to recalculate the distances and the rotation velocities according to

$$R = R_0 \sin l, \tag{3}$$

$$\Theta(R) = \Theta_0 \sin l + \Theta_{\rm tangent}\,. \tag{4}$$

The distances and radial velocities of the HII regions compiled by Fich et al. (1989) are used to recalculate the distances and rotation velocities using

$$R = (R_0^2 + d^2 - 2R_0 d\cos l)^{1/2}, \tag{5}$$

$$\Theta(R) = \left(\frac{\Theta_{\rm radial}}{R_0 \sin l \cos b} + \frac{\Theta_0}{R_0}\right) R\,. \tag{6}$$

Data from the HII regions within the range $l = 170^\circ\sim190^\circ$ are excluded to avoid large errors in the rotation velocities $\Theta(R)$ due to the $1/\sin l$ effect. We reprocess the data of Demers & Battinelli (2007) on the distances and radial velocities of C stars in the same way.

We also include the results of $W = \Theta(R/R_0) - \Theta_0$ and R/R_0 obtained by Merrifield (1992) and Honma & Sofue (1997) using the HI-disk thickness method and recalculate the distances and rotation velocities with the new Galactic constants by

$$R = R_0 \left(\frac{R}{R_0}\right), \tag{7}$$

$$\Theta(R) = \left(\frac{R}{R_0}\right)(W + \Theta_0)\,. \tag{8}$$

Finally, for the 43 HMSFRs from early VLBA, VERA and EVN observations, the distances to the GC and rotation velocities are obtained from the parallax and proper motion measurements of their masers, with the corresponding uncertainties estimated using a Monte Carlo method. The results are shown in Table 1. We also delineate the derivation procedure in Appendix A.

It is apparent that the measured rotation curve for the Milky Way shown in Figure 1 rises from 3 kpc to 10 kpc and then rises further in the outer Galaxy beyond 15 kpc. We also notice large discrepancies between the HMSFR data, which tend to define a flatter rotation curve, and other target objects at Galactocentric distances beyond 10 kpc. These discrepancies require further investigation using VLBI observation.

3 MASS MODEL OF THE MILKY WAY AND FITTING THE ROTATION CURVE

Generally speaking, two types of models have been used to interpret the flat outer rotation curves of galaxies. One class of models, of which modified Newtonian dynamics (MOND; Bekenstein & Milgrom 1984; Bienaymé et al. 2009) is the best-known example, claims that Newton's law of gravitation is not valid at large scale. In the other, and more widely-accepted, class of models, conventional gravitational theory is used with a dark matter distribution serving to explain the flat rotation

Table 1 Rotation Curve Data of 43 HMSFRs

Source	R (kpc)	$\Theta(R)$ (km s^{-1})	Observation facility	Ref.
G 23.0–0.4	4.546±0.248	222.61±6.10	VLBA	[16]
G 23.4–0.2	3.807±0.478	221.53±19.21	VLBA	[16]
G 23.6–0.1	5.622±0.336	255.93±4.24	VLBA	[16]
G 35.2–0.7	6.728±0.155	240.07±3.47	VLBA	[16]
G 35.2–1.7	6.032±0.295	236.44±7.34	VLBA	[16]
W 51 IRS 2	6.395±1.141	241.67±26.15	VLBA	[16]
G 59.7+0.1	7.547±0.026	247.18±2.95	VLBA	[16]
Cep A	8.663±0.016	241.89±4.73	VLBA	[16]
NGC 7538	9.689±0.072	222.54±2.75	VLBA	[16]
IRAS 00420	9.686±0.061	232.20±3.70	VLBA	[16]
NGC 281	10.201±0.181	252.44±4.09	VERA	[16]
W3(OH)	9.856±0.030	235.78±3.39	VLBA	[16]
WB 89–437	13.331±0.194	253.50±12.77	VLBA	[16]
S 252	10.480±0.026	238.32±0.56	VLBA	[16]
S 269	13.555±0.456	253.01±1.85	VERA	[16]
Orion	8.742±0.005	243.31±2.83	VERA	[16]
G 232.6+1.0	9.512±0.072	242.55±3.25	VLBA	[16]
VY CMa	9.035±0.051	239.13±2.75	VERA	[16]
AFGL 2591	8.419±0.023	235.28±4.88	VLBA	[10]
AFGL 2789	9.170±0.125	217.56±7.05	VERA	[10]
DR 20	8.294±0.002	237.86±4.99	EVN	[10]
DR 21	8.318±0.003	238.37±4.97	EVN	[10]
G 9.62+0.20	3.428±0.565	194.32±15.60	VLBA	[11]
G 14.33–0.64	7.320±0.130	253.30±7.66	VERA	[13]
G 15.03–0.68	6.508±0.124	254.02±1.92	VLBA	[15]
G 34.43+0.24	7.165±0.094	279.99±6.39	VERA	[5]
G 75.30+1.32	10.806±0.287	243.64±8.73	VLBA	[12]
IRAS 05137+3919	19.921±3.040	211.53±40.57	VERA	[3]
IRAS 06058+2138	10.140±0.468	234.82±7.77	VERA	[8]
IRAS 06061+2151	10.397±0.128	225.53±2.26	VERA	[7]
IRAS 19213+1723	6.732±0.306	235.42±10.70	VERA	[8]
IRAS 19312+1950	6.980±0.119	235.71±8.90	VERA	[4]
IRAS 20126+4104	8.221±0.001	233.58±5.03	VLBA & EVN	[6]
IRAS 20290+4052	8.267±0.002	238.90±4.97	EVN	[10]
K 3-35	7.022±0.066	227.78±5.26	VERA & VLBA	[14]
L 1206	8.672±0.039	238.30±3.48	EVN	[9]
L 1287	8.918±0.020	235.35±2.42	EVN	[9]
L 1448C	8.601±0.016	230.28±3.99	VERA	[2]
NGC 281-W	9.888±0.088	250.65±2.67	EVN	[9]
ON 1	7.881±0.010	240.72±5.03	EVN	[9]
ON 2N	8.341±0.116	240.69±5.85	VERA	[1]
S 255	9.960±0.069	250.39±11.76	EVN	[9]
W 75N	8.316±0.001	250.41±5.00	EVN	[10]

[1] Ando et al. (2011); [2] Hirota et al. (2011); [3] Honma et al. (2011); [4] Imai et al. (2011); [5] Kurayama et al. (2011); [6] Moscadelli et al. (2011); [7] Niinuma et al. (2011); [8] Oh et al. (2010); [9] Rygl et al. (2010); [10] Rygl et al. (2012); [11] Sanna et al. (2009); [12] Sanna et al. (2012); [13] Sato et al. (2010); [14] Tafoya et al. (2011); [15] Xu et al. (2011); [16] Reid et al. (2009b) and references therein.

curves. In the present paper, we assume that dark matter exists and try to constrain the dark matter halo from the new rotation curve of the Milky Way.

Modeling the mass distribution of the Milky Way has been done by many researchers. Three of them merit particular attention. Dehnen & Binney (1998) established a parameterized mass model of the Milky Way and fitted it to the available observational constraints, such as the terminal velocities,

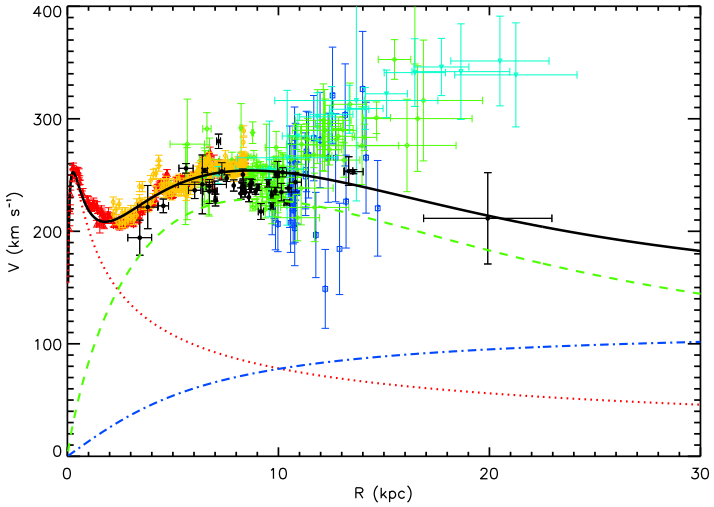

Fig. 1 Recalculated rotation data of the Milky Way using the new Galactic constants $(R_0, \Theta_0) = (8.4\ \mathrm{kpc}, 254\ \mathrm{km\ s^{-1}})$, with the rotation curve corresponding to Fit #1 (*thick solid line*). The dotted, dashed and dash-dotted lines represent the bulge, disk and dark matter halo contributions respectively. Red triangles: HI- and CO-line tangent velocity method (Clemens 1985); yellow open circles: HI tangent velocity method (Fich et al. 1989); green diamonds: HII regions (Fich et al. 1989); blue squares: C stars (Demers & Battinelli 2007); cyan reverse triangles: HI-disk thickness method (Merrifield 1992; Honma & Sofue 1997); black filled circles: HMSFR data (Ando et al. 2011; Hirota et al. 2011; Honma et al. 2011; Imai et al. 2011; Kurayama et al. 2011; Moscadelli et al. 2011; Niinuma et al. 2011; Oh et al. 2010; Rygl et al. 2010; Rygl et al. 2012; Sanna et al. 2009; Sanna et al. 2012; Sato et al. 2010; Tafoya et al. 2011; Xu et al. 2011 and Reid et al. 2009b).

Oort's constants, the local surface density of the disk and a limited amount of the rotation curve data of the outer Galaxy. Weber & de Boer (2010) used the same method to study the dark matter density distribution of the Milky Way. Sofue et al. (2009), on the other hand, took their mass model to directly fit the unified rotation curve of the Milky Way. Here we adopt a three-component mass model similar to that of Sofue et al. (2009).

3.1 Function Forms of the Mass Model

The overall rotation velocity of the Milky Way is contributed by three components: the bulge, disk and halo, and is calculated as

$$\Theta_{\rm t}(R)^2 = \Theta_{\rm b}^2(R) + \Theta_{\rm d}^2(R) + \Theta_{\rm h}^2(R)\,. \tag{9}$$

3.1.1 Spherical bulge

We adopt the spherical Hernquist model (Hernquist 1990) for the bulge, which produces the rotation velocity given by

$$\Theta_{\rm b}^2(R) = \frac{GM_{\rm b}R}{(R+R_{\rm b})^2}\,, \tag{10}$$

in which $M_{\rm b}$ is the total mass of the bulge and $R_{\rm b}$ is its scale radius.

3.1.2 Exponential disk

According to Binney & Tremaine (2008), a disk with surface mass density $\Sigma(r)$ contributes to the rotation velocity as

$$\Theta^2(R) = -4G \int_0^R \mathrm{d}a \frac{a}{\sqrt{R^2-a^2}} \frac{\mathrm{d}}{\mathrm{d}a} \int_a^\infty \mathrm{d}r \frac{r\Sigma(r)}{\sqrt{r^2-a^2}} \,. \tag{11}$$

Since

$$\frac{\mathrm{d}}{\mathrm{d}a} \int_a^\infty \mathrm{d}r \frac{r\Sigma(r)}{\sqrt{r^2-a^2}} = a \int_a^\infty \frac{\Sigma^{'}(r)\mathrm{d}r}{\sqrt{r^2-a^2}}$$

(Gorenflo & Vessella 1991), the rotation velocity for the disk is

$$\Theta^2(R) = -4G \int_0^R \mathrm{d}a \frac{a^2}{\sqrt{R^2-a^2}} \int_a^\infty \frac{\Sigma^{'}(r)\mathrm{d}r}{\sqrt{r^2-a^2}} \,. \tag{12}$$

Equation (12) can be used to compute the rotation velocity of any mass component with an axisymmetric mass distribution.

We adopt an exponential disk model with surface mass density

$$\Sigma_\mathrm{d}(r) = \Sigma_\mathrm{dc} \exp\left(-r/R_\mathrm{d}\right), \tag{13}$$

where Σ_dc is the central surface mass density and R_d is the scale radius. The mass of the disk is

$$M_\mathrm{dt} = 2\pi R_\mathrm{d}^2 \Sigma_\mathrm{dc} \,. \tag{14}$$

Inserting Equation (13) into Equation (12), Binney & Tremaine (2008) give the rotation velocity as

$$\Theta_\mathrm{d}^2(R) = 4\pi G \Sigma_\mathrm{dc} R_\mathrm{d} y^2 \left[I_0(y)K_0(y) - I_1(y)K_1(y)\right] , \tag{15}$$

where $y = R/(2R_\mathrm{d})$.

3.1.3 Semi-isothermal spherical dark matter halo

There are many models for the dark matter halo. Sofue et al. (2009) show that within 20 kpc, different dark matter halo models tend to yield relatively similar results, so we simply adopt the semi-isothermal spherical dark matter halo model with density distribution

$$\rho(r) = \rho_\mathrm{hc} \left[1 + \left(\frac{r}{R_\mathrm{h}}\right)^2\right]^{-1} , \tag{16}$$

where ρ_hc and R_h are the central mass density and scale radius, respectively. The mass of the dark matter halo within radius R is

$$M_\mathrm{h}(R) = \int_0^R \rho(r) \cdot 4\pi r^2 \mathrm{d}r = 4\pi \rho_\mathrm{hc} R_\mathrm{h}^2 R \left[1 - \frac{R_\mathrm{h}}{R} \arctan\left(\frac{R}{R_\mathrm{h}}\right)\right] , \tag{17}$$

thus giving the rotation velocity as

$$\Theta_\mathrm{h}^2(R) = \frac{GM_\mathrm{h}(R)}{R} = \Theta_\infty^2 \left[1 - \frac{R_\mathrm{h}}{R} \arctan\left(\frac{R}{R_\mathrm{h}}\right)\right] , \tag{18}$$

where $\Theta_\infty = \sqrt{4\pi G \rho_\mathrm{hc} R_\mathrm{h}^2}$.

3.2 Fitting the Mass Model

We construct the model of the Milky Way with six free parameters, $M_{\rm b}$, $R_{\rm b}$, $\Sigma_{\rm dc}$, $R_{\rm d}$, $\rho_{\rm hc}$ and $R_{\rm h}$. We evaluate the values of these parameters using nonlinear fitting to minimize χ^2 in the form of the reduced χ^2,

$$\chi^2/\nu = \frac{1}{N-p-1}\sum_{N}\left\{\omega_i\left[\Theta_i^{\rm o}(R)-\Theta_i^{\rm m}(R)\right]^2\right\}, \quad (19)$$

where $N = 521$ is the total number of data to be fitted, $p = 6$ is the number of free parameters and $\Theta_i^{\rm o}(R)$ and $\Theta_i^{\rm m}(R)$ denote the observed and modeled rotation velocity at Galactocentric distance R, respectively. The weight ω_i for each data point is taken as its inverse error squared $\omega = 1/\sigma_i^2$. The data with large error bars do not generally affect the trend of the rotation curves but worsen the values of the fitting statistic.

One of the sources of the 43 HMSFRs, IRAS 05137+3919 (represented by the outermost black filled circle and error bar in Fig. 1), is one of the most distant star-forming regions from the GC observed by Honma et al. (2011), and has quite an unusually large error and thus is ignored during the fitting process.

In our fitting, we adjust the six free parameters so as to best match the rotation curve data by means of the standard particle swarm optimization (SPSO) algorithm (Kennedy & Eberhart 1995). Three sets of fitting results are listed in Table 2, as well as the fitted rotation curves shown in Figures 1 and 2.

The best fit is Fit #1 with $\chi^2/\nu = 10.4$. In this fit the rotation curve falls beyond 15 kpc. Several fits with similar values of χ^2/ν, such as Fits #2 and #3, can also be constructed by increasing the central mass density of the dark matter halo, which results in the flatter outer rotation curves shown in Figure 3. The three fits produce similar parameters for the inner bulge component, but vary in their results for the disk and halo components because of a certain degree of degeneracy between the parameters describing the disk and halo components.

Table 2 Fitting Parameters for the Milky Way Model

No.	Reduced χ^2 value	Component	Parameter	Value
		Bulge	Total mass	$M_{\rm b}$ =1.49×10^{10} $M_\odot$
			Scale radius	$R_{\rm b}$ = 0.26 kpc
Fit #1	10.4	Disk	Scale radius	$R_{\rm d}$ = 4.14 kpc
			Central mass density	$\Sigma_{\rm dc}$ = 1.21×10^3 $M_\odot$ pc^{-2}
		Dark matter halo	Scale radius	$R_{\rm h}$ = 5.0 kpc
			Central volume mass density	$\rho_{\rm hc}$ = 0.01 $M_\odot$ pc^{-3}
		Bulge	Total mass	$M_{\rm b}$ =1.49×10^{10} $M_\odot$
			Scale radius	$R_{\rm b}$ = 0.26 kpc
Fit #2	10.6	Disk	Scale radius	$R_{\rm d}$ = 3.89 kpc
			Central mass density	$\Sigma_{\rm dc}$ = 1.15×10^3 $M_\odot$ pc^{-2}
		Dark matter halo	Scale radius	$R_{\rm h}$ = 5.0 kpc
			Central volume mass density	$\rho_{\rm hc}$ = 0.02 $M_\odot$ pc^{-3}
		Bulge	Total mass	$M_{\rm b}$ =1.48×10^{10} $M_\odot$
			Scale radius	$R_{\rm b}$ = 0.25 kpc
Fit #3	11.0	Disk	Scale radius	$R_{\rm d}$ = 3.51 kpc
			Central mass density	$\Sigma_{\rm dc}$ = 1.10×10^3 $M_\odot$ pc^{-2}
		Dark matter halo	Scale radius	$R_{\rm h}$ = 5.5 kpc
			Central volume mass density	$\rho_{\rm hc}$ = 0.03 $M_\odot$ pc^{-3}

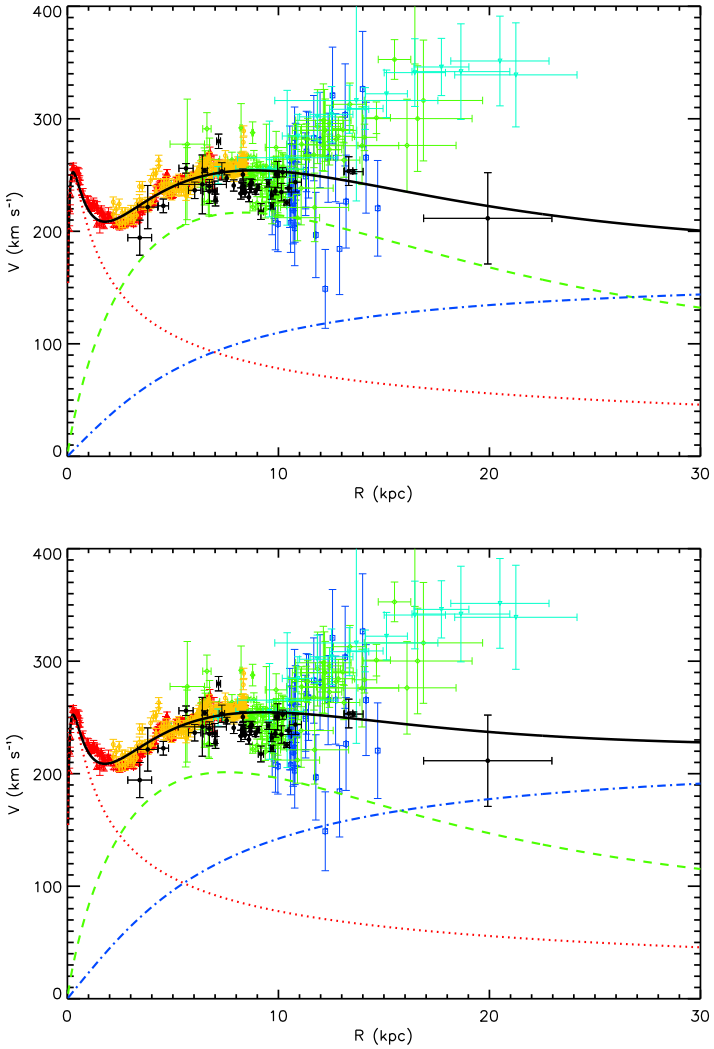

Fig. 2 Alternative model rotation curves of the Milky Way with the data and model components represented as in Fig. 1. *Upper*: Fit #2. *Lower*: Fit #3.

4 DISCUSSION

Present-day VLBI parallax and proper motion measurements with accuracies of $\sim$10 μas and $\sim$1 km s^{-1}, respectively, have allowed us to construct an accurate rotation curve of the Milky Way. We tentatively made a new rotation curve of the Milky Way using the existing data in the literature and the first measurements of the trigonometric parallaxes and proper motions with VLBA, VERA and EVN. We found that the rotation curve of the Milky Way is nearly flat or slightly rising in the region from about 6 to 15 kpc. The rotation velocities within 5 kpc of the GC determined by VLBI are apparently different from those obtained by the measurement of the HI- and CO-line tangent velocities. The rotation curve appears to drop slowly beyond $\sim$15 kpc, although the only VLBI

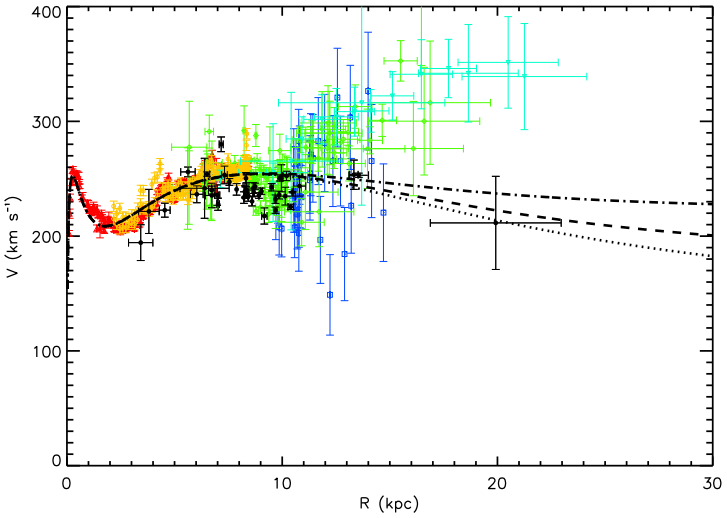

Fig. 3 The rotation curves of the three fits plotted together for comparison. The dotted, dashed and dash-dotted lines correspond to Fits #1, #2 and #3, respectively. The inner rotation curves of the three fits are very similar, but the outer parts start to rise as the central mass density of the dark matter halo increases from Fit #1 to Fit #3.

measurement corroborating this decline is for IRAS 05137+3919, which has a large error bar and is excluded in our fitting.

It is evident that the fitting results from the first VLBI data combined with the existing data in the literature are far from satisfactory. There are three possible problems.

Firstly, the rotation curve data are produced from a range of methods and sources. On the one hand, this enables us to obtain a unified view of the kinematics of the Milky Way, but on the other hand, it also creates challenges. The dispersive nature of the data manifested in Figure 1 makes it difficult to acquire accurate and consistent numerical fitting results - indeed, Sofue et al. (2009) only obtained the fitting results through trial and error by means of eye estimate and gave an uncertainty at the 5% $\sim$ 10% level. In particular, the data obtained using the methods of HI-disk thickness and C stars have a relatively large uncertainty. If we discard those data with large error bars, the undersampling problem of the remaining data, which mainly occupy the region inside 10 kpc of the rotation curve, also hinders the process of fitting and no better results are yielded. This problem could be solved by the BeSSeL project if it can provide more data in the outer 10 kpc $\sim$ 20 kpc of the Milky Way. More epochs of the measurements of parallaxes and proper motions are needed to improve the accuracies of distance and rotation velocity for the sources far from the GC, such as IRAS 05137+3919.

Secondly, our choice of mass model may be inadequate for the estimation of the parameters of the Milky Way. A good model requires a thorough understanding of the mass distribution of the Milky Way, but the most appropriate choice is still unclear.

Finally, it can be seen from both Figure 1 and our fitting results in Table 2 that the data corresponding to the outer Galaxy, i.e. 15 kpc and beyond, are scarce and thus have poorly constrained the model parameters related to the dark matter halo. The uncertainty in the determination of the dark matter halo, in turn, affects the fitting result of the disk.

Using the fitting results of our mass model, we manage to determine some of the parameters of the Milky Way, which are listed in Table 3. It is worth mentioning that the dark matter halo

Table 3 Estimated Parameters of the Milky Way Model

Component	Parameter	Value
Bulge	Half-mass scale radius	$R_{\rm b} \sim 0.3$ kpc
	Mass	$M_{\rm b} \sim 1.5\times10^{10}\ M_\odot$
Disk	Scale radius	$R_{\rm d} \sim 4.0$ kpc
	Central mass density	$\Sigma_{\rm dc} \sim 1.2\times10^{3}\ M_\odot$ pc^{-2}
	Mass	$M_{\rm d} \sim 1.2\times10^{11}\ M_\odot$
Dark matter halo	Scale radius	$R_{\rm h} \sim 5.0$ kpc
	Central volume mass density	$\rho_{\rm hc} \sim 0.01\ M_\odot$ pc^{-3}
	Mass in $r = 20$ kpc sphere	$M_{\rm h}$ (20 kpc) = $1.0\times10^{11}\ M_\odot$
Total Galaxy mass	Mass in $r = 20$ kpc sphere	$M_{\rm total}$ (20 kpc) = $2.3\times10^{11}\ M_\odot$

mass within 20 kpc amounts to $10^{11}\ M_\odot$. We believe that because our data for the outer Galaxy are inadequate, the determination of the mass of the halo is somewhat conservative. Moreover, the mass of the entire Galaxy is around $2.3\times10^{11}\ M_\odot$ (20 kpc) which is about 10% larger than that from Sofue et al. (2009) and comparable with the mass of M31, $3.4\times10^{11}\ M_\odot$ (35 kpc) (Carignan et al. 2006).

For the dark matter distribution in the Milky Way, we only attempt with the semi-isothermal dark matter halo model. Many other analytic models and simulations of the dark matter exist in the literature. Weber & de Boer (2010) summarize that dark matter substructure, such as dark matter disks and rings, can be other alternative explanations for the dips in the rotation curve. Recent observations also indicate the existence of such dark matter substructures, suggesting an even larger mass for the dark matter halo than what we find in our fits.

5 CONCLUSIONS

We have presented the revised Galactic rotation curve using observation data from the literature and the most up-to-date accurate VLBI data with new Galactic constants $(R_0, \Theta_0) = (8.4\ \mathrm{kpc}, 254\ \mathrm{km\,s^{-1}})$. From the limited VLBI maser astrometry data, we find that the rotation curve of the Milky Way is almost flat or slightly rising at Galactocentric distances of approximately 6 to 15 kpc. The rotation velocities within 5 kpc of the GC determined by VLBI are apparently different from those obtained by measurement of the HI- and CO-line tangent velocities. By using the spherical bulge, exponential disk and semi-isothermal dark matter halo model of the Galaxy, we fit our new rotation curve and obtain the mass distribution and structure parameters of the Milky Way, which are shown in Table 3. Due to the new Galactic constants we adopt, the total mass (20 kpc) of the Milky Way we obtain from the fitting is about 10% larger than that from Sofue et al. (2009) and is comparable to that of M31 (Carignan et al. 2006), confirming the suggestions of Reid et al. (2009b), where the interpretation of the similarities of the rotation curves of the Milky Way and M31 is that these two galaxies are nearly equal in size and mass.

Our model of the Milky Way is constrained to axisymmetric components, whereas spiral arms and the central bar are also important features of the Milky Way that need to be added to the model in future work. The VLBA BeSSeL project will hopefully observe a large number of maser sources in the Milky Way, thus providing us with a much improved view of the three-dimensional structure of the Milky Way. This will certainly enable us to create more accurate and detailed rotation curves and learn more about the mass distribution of the Milky Way.

Acknowledgements We would like to thank Rui-Zhu Chen and Xiang-Yu Ma for their numerical support in the work. We are also grateful to Prof. Mark Birkinshaw for his kind help. This work was supported by the National Natural Science Foundation of China (Grant Nos. 11133008 and J1210039).

Appendix A: DERIVATION OF GALACTIC ROTATION PARAMETERS FROM PARALLAXES AND PROPER MOTIONS

We basically follow the procedure outlined by Reid et al. (2009b). The source parameters are listed in Table A.1 and the planar Galactic geometry and some of the parameters are depicted in Figure A.1. The position (α and δ), distance relative to the Sun ($\pi_{\rm s}$ or D), LSR velocity ($v_{\rm LSR}$) and proper motions (μ_α and μ_δ) of each source are all given by the measurements. The Galactic and solar parameters relevant to the derivation are summarized in Table A.2.

Table A.1 Source Parameter Definitions

Parameter	Definition
α	Right ascension
δ	Declination
l	Galactic longitude
b	Galactic latitude
D	Distance from the Sun ($1/\pi_{\rm s}$)
$D_{\rm p}$	Distance from the Sun projected in plane
$R_{\rm p}$	Distance from the GC projected in plane
$v_{\rm LSR}$	LSR radial velocity
$v_{\rm helio}$	Heliocentric radial velocity
μ_α	Proper motion in R.A.
μ_δ	Proper motion in Decl.
μ_l	Proper motion in Galactic longitude
μ_b	Proper motion in Galactic latitude
β	Angle: Sun–GC–source

GC: Galactic center; LSR: local standard of rest; NGP: north galactic pole.

Table A.2 The Galactic and Solar Parameters and Nominal Values

Parameter	Value	Definition
R_0	8.4 kpc	Distance to the GC of the Sun
Θ_0	254 km s^{-1}	Galactic rotation velocity at the Sun
$U_\odot^{\rm Std}$	10.3 km s^{-1}	Standard solar motion toward GC
$V_\odot^{\rm Std}$	15.3 km s^{-1}	Standard solar motion toward $l = 90^\circ$
$W_\odot^{\rm Std}$	7.7 km s^{-1}	Standard solar motion toward NGP
$U_\odot^{\rm H}$	10.0 km s^{-1}	Hipparcos solar motion toward GC
$V_\odot^{\rm H}$	5.2 km s^{-1}	Hipparcos solar motion toward $l = 90^\circ$
$W_\odot^{\rm H}$	7.2 km s^{-1}	Hipparcos solar motion toward NGP

GC: Galactic center; NGP: north galactic pole. The values are taken from Reid et al. (2009b) and reference therein.

Firstly, we transform $v_{\rm LSR}$ to the heliocentric frame $v_{\rm helio}$ by adding back the component of the standard solar motion in the line-of-sight direction

$$v_{\rm helio} = v_{\rm LSR} - (U_\odot^{\rm Std}\cos l + V_\odot^{\rm Std}\sin l)\cos b - W_\odot^{\rm Std}\sin b\,. \quad \text{(A.1)}$$

Secondly, we convert the proper motions in the equatorial heliocentric frame (μ_α, μ_δ) to those in the Galactic heliocentric frame (μ_l, μ_b). The transformation from the equatorial coordinate system

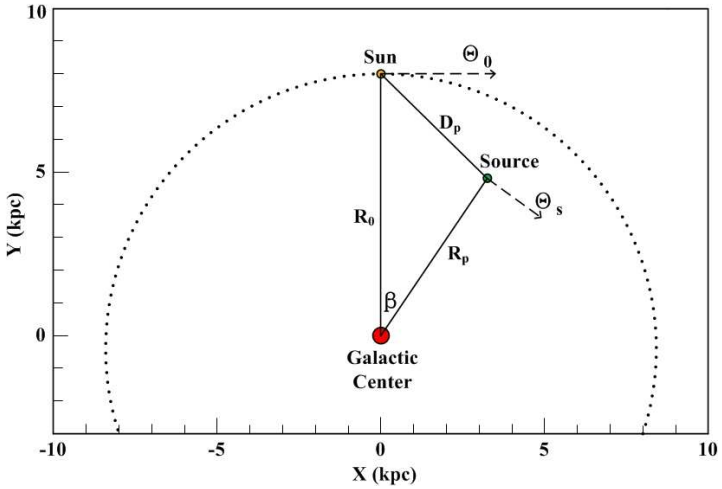

Fig. A.1 Schematic sketch of planar Galactic geometry and parameters.

(α, δ) to the Galactic coordinate system (l, b) is

$$\sin b = \sin\delta\cos(90^\circ - \delta_P) - \cos\delta\sin(\alpha - \alpha_P - 6^h)\sin(90^\circ - \delta_P), \quad \text{(A.2)}$$

$$\sin\phi = \big(\cos\delta\sin(\alpha - \alpha_P - 6^h)\cos(90^\circ - \delta_P) + \sin\delta\sin(90^\circ - \delta_P)\big)/\cos b, \quad \text{(A.3)}$$

$$\cos\phi = \cos\delta\cos(\alpha - \alpha_P - 6^h)/\cos b\,, \quad \text{(A.4)}$$

where l is related to ϕ by

$$l = \phi + (\theta - 90^\circ)\,. \quad \text{(A.5)}$$

The right ascension $\alpha_P = 12^{\rm h}51^{\rm m}26.2817^{\rm s}$ and declination $\delta_P = 27^\circ07'42.013''$ of the NGP and the angle $\theta = 122.932^\circ$ are taken from Reid et al. (2009b). Then the proper motion in Galactic coordinates (μ_l, μ_b) can be obtained by taking the difference of the coordinates (l, b) one year apart, which is computed using the above transformation equations taking into account the proper motion in equatorial coordinates (μ_α, μ_δ). The linear velocities are calculated in turn via

$$v_l = D\mu_l\cos b \ \text{ and } \ v_b = D\mu_b\,. \quad \text{(A.6)}$$

Thirdly, velocity transformation between spherical and Cartesian Galactic coordinates at the Sun is carried out

$$\begin{aligned} U_1 &= (v_{\rm helio}\cos b - v_b\sin b)\cos l - v_l\sin l, \\ V_1 &= (v_{\rm helio}\cos b - v_b\sin b)\sin l + v_l\cos l, \\ W_1 &= v_b\cos b + v_{\rm helio}\sin b\,. \end{aligned} \quad \text{(A.7)}$$

Fourthly, we add the full orbital motion of the Sun $(U_\odot^{\rm H}, V_\odot^{\rm H} + \Theta_0, W_\odot^{\rm H})$ to produce the inertial velocities,

$$U_2 = U_1 + U_\odot^{\rm H}\ , \quad V_2 = V_1 + V_\odot^{\rm H} + \Theta_0\ , \quad W_2 = W_1 + W_\odot^{\rm H}\,. \quad \text{(A.8)}$$

Finally, the Galactocentric distance and the rotation velocity of the source are calculated. The distance R_p is

$$R_p^2 = R_0^2 + D_p^2 - 2R_0D_p\cos l\,, \quad \text{(A.9)}$$

where $D_p = D\cos b$. The corresponding rotation velocity is

$$\Theta_s = V_2 \cos\beta + U_2 \sin\beta\,. \tag{A.10}$$

The angle β is obtained from

$$\sin\beta = \frac{D_p}{R_p}\sin l \quad \text{and} \quad \cos\beta = \frac{R_0 - D_p\cos l}{R_p}\,. \tag{A.11}$$

The peculiar motions of the sources are neglected in the computation of the rotation velocities, which conforms with the treatment of other data samples for the Galactic rotation curve.

References

Ando, K., Nagayama, T., Omodaka, T., et al. 2011, PASJ, 63, 45
Bekenstein, J., & Milgrom, M. 1984, ApJ, 286, 7
Bienaymé, O., Famaey, B., Wu, X., Zhao, H. S., & Aubert, D. 2009, A&A, 500, 801
Binney, J., & Tremaine, S. 2008, Galactic Dynamics: Second Edition (Princeton University Press)
Brunthaler, A., Reid, M. J., Menten, K. M., et al. 2009, ApJ, 693, 424
Burton, W. B., & Gordon, M. A. 1978, A&A, 63, 7
Carignan, C., Chemin, L., Huchtmeier, W. K., & Lockman, F. J. 2006, ApJ, 641, L109
Clemens, D. P. 1985, ApJ, 295, 422
Dehnen, W., & Binney, J. 1998, MNRAS, 294, 429
Demers, S., & Battinelli, P. 2007, A&A, 473, 143
Fich, M., Blitz, L., & Stark, A. A. 1989, ApJ, 342, 272
Gorenflo, R., & Vessella, S. 1991, Abel Integral Equations: Analysis and Applications (Berlin: Springer-Verlag)
Hernquist, L. 1990, ApJ, 356, 359
Hirota, T., Honma, M., Imai, H., et al. 2011, PASJ, 63, 1
Honma, M., & Sofue, Y. 1997, PASJ, 49, 453
Honma, M., Hirota, T., Kan-Ya, Y., et al. 2011, PASJ, 63, 17
Imai, H., Tafoya, D., Honma, M., Hirota, T., & Miyaji, T. 2011, PASJ, 63, 81
Kennedy, J., & Eberhart, R. 1995, in Proceedings of IEEE International Conference on Neural Networks (Piscataway: IEEE Service Center), 4, 1942
Kurayama, T., Nakagawa, A., Sawada-Satoh, S., et al. 2011, PASJ, 63, 513
Merrifield, M. R. 1992, AJ, 103, 1552
Moscadelli, L., Reid, M. J., Menten, K. M., et al. 2009, ApJ, 693, 406
Moscadelli, L., Cesaroni, R., Rioja, M. J., Dodson, R., & Reid, M. J. 2011, A&A, 526, A66
Niinuma, K., Nagayama, T., Hirota, T., et al. 2011, PASJ, 63, 9
Oh, C. S., Kobayashi, H., Honma, M., et al. 2010, PASJ, 62, 101
Reid, M. J., Menten, K. M., Brunthaler, A., et al. 2009a, ApJ, 693, 397
Reid, M. J., Menten, K. M., Zheng, X. W., et al. 2009b, ApJ, 700, 137
Rygl, K. L. J., Brunthaler, A., Reid, M. J., et al. 2010, A&A, 511, A2
Rygl, K. L. J., Brunthaler, A., Sanna, A., et al. 2012, A&A, 539, A79
Sanna, A., Reid, M. J., Moscadelli, L., et al. 2009, ApJ, 706, 464
Sanna, A., Reid, M. J., Dame, T. M., et al. 2012, ApJ, 745, 82
Sato, M., Hirota, T., Reid, M. J., et al. 2010, PASJ, 62, 287
Sofue, Y., Honma, M., & Omodaka, T. 2009, PASJ, 61, 227
Tafoya, D., Imai, H., Gomez, Y., et al. 2011, PASJ, 63, 71
Weber, M., & de Boer, W. 2010, A&A, 509, A25
Xu, Y., Reid, M. J., Menten, K. M., et al. 2009, ApJ, 693, 413
Xu, Y., Moscadelli, L., Reid, M. J., et al. 2011, ApJ, 733, 25
Zhang, B., Zheng, X. W., Reid, M. J., et al. 2009, ApJ, 693, 419